Novel Modulation Concepts for a Drive-Integrated Auxiliary Dc-Dc Converter for Hybrid Vehicles

H. Plesko, J. Biela, J. W. Kolar
Power Electronic Systems Laboratory
Swiss Federal Institute of Technology (ETH)
ETH Zentrum, ETL
8092 Zurich, Switzerland
Email: plesko@lem.ee.ethz.ch

***Abstract*—Hybrid vehicles are a characteristic feature of the daily traffic yet, with growing fuel costs and other factors increasing their importance in the nearest future even more. Nevertheless, hybrid vehicles are not a mass product up to now. Although the life cycle costs of the hybrid cars are usually smaller than the costs for comparable fuel vehicles, the main purchase criteria for vehicles are still the acquisition costs, leading to a preference for conventional fuel cars. So as to increase the number of hybrid vehicles, the production costs have to be lowered.In hybrid vehicles, the energy distribution system causes a significant share of volume and costs. One part of this system is the dc-dc converter that transfers power between the low- and high-voltage buses. In order to reduce the costs and the volume of this converter, two new concepts for integrating the dc-dc converter functionality into the traction drive system have been presented in [1]. This paper will present different switching strategies to improve the efficiency of the total system. Starting from the phase-shift modulation known from the conventional Dual Active Bridge, the switching instants are optimized regarding efficiency to obtain the optimal modulation. In addition, a concept with multiple switching during the inverter's switching period is analyzed as well as a slightly modified system, where one leg of the dc-dc converter is implemented as a three-level switch. These four switching strategies are analyzed and compared. In addition, measurement results are shown to verify the calculations.**

I. Introduction

Rising fuel costs and an increasing environmental consciousness give rise to a growing interest in hybrid vehicles. Nevertheless, hybrid vehicles are not a mass product up to now. To increase the number of hybrid vehicles, the production costs have to be lowered.

Conventional mild and full hybrid electric vehicles usually have two different voltage levels. The 14 V dc bus with the traditional loads such as fans and lighting systems is often supplied by a 12 V battery. Another high-voltage 200 V...600 V dc bus provides the necessary power for the propulsion system, and is connected to the low-voltage bus via a bidirectional dc-dc converter. As the power ratings for the propulsion system are relatively high, it would be desirable for mild and full hybrids to feed the propulsion system from the high-voltage bus [2]. Therefore, the dc-dc converter needs to have a galvanic isolation for safety reasons. The electric machine is supplied by a three phase dc-ac converter connected to the high-voltage bus.

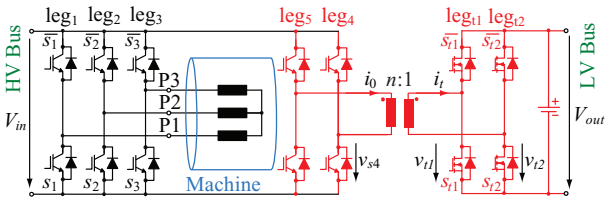

(a) Separated dc-dc converter and inverter

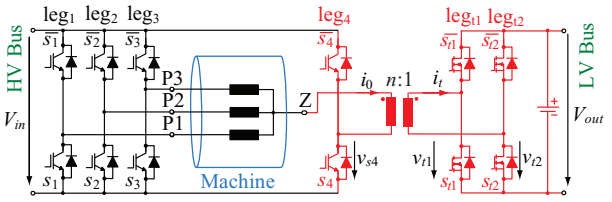

(b) Proposed integrated dc-dc converter: MFCS-I

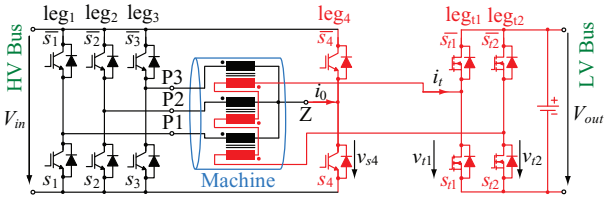

(c) Proposed integrated dc-dc converter: MFCS-II

Figure 1: Multi Functional Converter Systems (MFCS).

978-1-422-2812-0/09/$25.00 ©2009 IEEE

In order to reduce the costs of the electric system and increase the power density for decreasing the total production costs of the hybrid vehicle, the dc-dc converter linking the low- and high-voltage bus could be functionally integrated into the inverter and/or electric machine. There are mainly two types of integration. In a first step, the motor's zero-phase system could be utilized. For example, in [3] a possible integration of the dc-dc converter in the inverter system is presented, but it is applicable only for split-phase motors. Another integration possibility is described in [4], which is, however, not galvanically isolated since the high-voltage bus is omitted and the electrical machine is fed from 42 V. In addition, the output voltage V_{out} of the dc-dc converter cannot be controlled in every operating region of the drive system. If the inverter operates for example in the six-step mode, the switching state of the inverter is totally determined. There is no degree of freedom for controlling the output voltage. Similar concepts without galvanic isolation have been presented in [5], [6], [7], and [8]. In a second step, the motor's iron could be used additionally for integrating the transformer as presented in [9] and [10], but these systems are relative voluminous since they need a three-phase rectifier.

In summary, it would be ideal if the high-voltage to low-voltage dc-dc converter has a galvanic isolation, is controllable in all operating regions and has a single-phase rectifier. To achieve these requirements, two integrated high-voltage to low-voltage dc-dc converters with galvanic isolation have been proposed in [1] and [11]. Depending on the design, these converters can be used to transfer power bidirectionally between the 200...600 V and the 14 V or 42 V bus. The starting point is a conventional Dual Active Bridge (DAB) feeding a high-frequency transformer (see Figure 1(a)), whose output is rectified to the output voltage V_{out}. The secondary-side rectifier could be a conventional full-bridge configuration, or a diode rectifier, if only unipolar power transfer is required.

In the first concept, the fifth leg (i.e. leg_5 in Figure 1(a)) of the conventional system is replaced by using the zero-sequence voltage. There, the transformer is connected between the star point and the midpoint of the primary-side leg four (see Figure 1(b)). This concept is referred to as the Multi Functional Converter System I (MFCS-I) [12] in the following. In the second concept, the iron core of the motor is used for integrating the transformer as shown in Figure 1(c). Compared to the conventional machine, there is an additional secondary winding for each phase. As these secondary windings are connected in series, the total voltage appearing at the secondary side is proportional to the zero-sequence voltage of the machine in the no-load case minus the voltage across switch $s4$. This concept is referred to as the Multi Functional Converter System II (MFCS-II) [13]. Further details on both the systems are given in [1] and [11].

In this paper, new modulation strategies for these two systems, the Multi Functional Converter System I and II (MFCS-I and MFCS-II) are presented in order to reduce the rms currents and thus the losses. In **Subsection II**, the basic operating principle of the MFCS-I and the MFCS-II is shortly explained by introducing an equivalent circuit for the dc-dc converter. A more detailed analysis in **Subsection II-A** focuses on new modulation schemes to improve the efficiency. The theoretical results, including simulations, are verified experimentally using a 9.4 kW prototype in **Section II-B**.

II. Basic Principle of Operation

Both concepts MFCS-I and MFCS-II are based on the utilization of the zero-sequence voltage v_z and the zero-sequence impedance of the inverter/motor system. The zero-sequence voltage can be calculated by $v_z = \frac{V_{in}}{3}(\overline{s_1} + \overline{s_2} + \overline{s_3})$ where $\overline{s_\nu} = 1$ if switch $\overline{s_\nu}$ is closed and switch s_ν open and $\overline{s_\nu} = 0$ if $\overline{s_\nu}$ is open and s_ν closed (see Figure 1). V_{in} denotes the input voltage. The operation of the machine is not influenced by the integrated dc-dc converter because the zero-sequence flux does not contribute to the momentum.

The MFCS-I shown in Figure 1(b) takes advantage of the zero-sequence voltage to save one leg compared to the conventional system shown in Figure 1(a). The integrated dc-dc converter of the MFCS-I can be modeled as shown in Figure 2(a). The time dependent voltage source v_z represents the zero-sequence voltage and v_{s4} describes the voltage across the switch s_4 (see Figure 1(b)). These two voltage sources

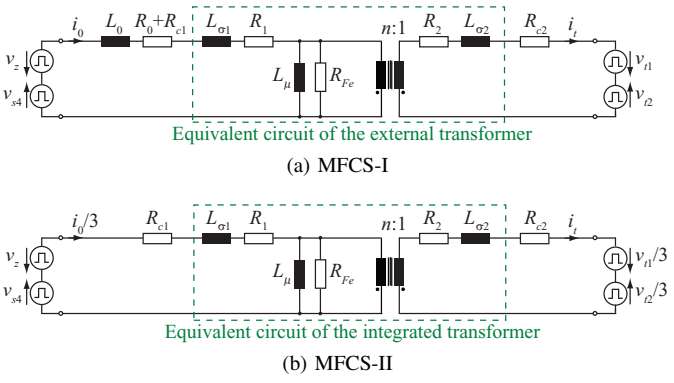

(a) MFCS-I

(b) MFCS-II

Figure 2: Equivalent circuit for the dc-dc converter.

are connected to a circuit similar to a transformer equivalent circuit. Voltages v_{t1} and v_{t2} represent the secondary voltages across switches s_{t1} and s_{t2} (see Figure 1(b)). R_0 and L_0 represent the machine's zero-sequence resistance and inductance, respectively. The IGBT and MOSFET losses and all other ohmic losses in the inverter are included in R_{c1} and R_{c2}. The transformer is defined by its frequency dependent winding resistances R_1 and R_2 and the leakage inductances $L_{\sigma1}$ and $L_{\sigma2}$. L_μ and R_{Fe} represent the external transformers magnetizing inductance and iron resistance.

In the second integration concept, the MFCS-II, the galvanic isolation is also integrated into the motor (see Figure 1(c) in order to reduce the costs and the weight further. To do so, additional windings must be placed in the slots together with the conventional winding. Since the secondary windings are connected in series, the positive- and negative-sequence voltages, fluxes etc. add up to zero and the only relevant part for the dc-dc converter of the inverter-machine subsystem is the zero-sequence impedance and the zero-sequence voltage v_z. Thus, the integrated dc-dc converter of the MFCS-II can be modeled as three transformers, where each therefrom has an equivalent circuit as shown in Figure 2(b). The voltages are the same as defined for the MFCS-I, but since the secondary windings of these three transformers are connected in series, only $v_{t1}/3$ and $v_{t2}/3$ are included. Similarly, only $i_0/3$ is included in one transformer since the primary side windings are connected in parallel. The IGBT and MOSFET losses and all other ohmic losses in the inverter are again included in R_{c1} and R_{c2}. R_1 and R_2 represent the winding resistances and $L_{\sigma1}$ and $L_{\sigma2}$ the stray inductances of the integrated transformer. L_μ and R_{Fe} are the integrated transformer's magnetizing inductance and iron resistance. Since the transformer is integrated into the motor in the MFCS-II, it is important to notice that the zero-sequence impedance corresponds to the transformer's primary side open-circuit impedance. Neglecting R_{Fe}, R_1 corresponds to the motor's zero-sequence resistance, $L_{\sigma1}$ to $1-k$ times and L_μ to k times the zero-sequence inductance where k is the coupling factor. Nevertheless, the equivalent circuits for both concepts are similar, thus allowing for a combined analysis.

A. *Control*

Since the MFCSs are based on the Dual Active Bridge concept, the phase-shift modulation has also been implemented for this system. However, the efficiency is rather poor for smaller output powers as the reactive power related to the output power is higher for these operating points. Therefore, it is desirable to improve the modulation strategy.

Table I: Constraints for the switching schemes.

Constraints for the switching schemes

- $v_z - v_{s4}$ has zero-mean related to one inverter switching period
- $v_{t1} - v_{t2}$ has zero-mean related to one inverter switching period
- Transferred power corresponds to the required power

As shown above, the main inductance L_μ of the MFCS-II in Figure 2(b) corresponds only to a part of the zero-sequence inductance, namely to kL_0 where k is the coupling factor of the integrated transformer. Similarly, the stray inductance $L_{\sigma1}$ corresponds to $(1-k)L_0$. For efficient motor operation, the zero-sequence inductance is usually rather small and hence also the stray and magnetizing inductance of the integrated transformer are rather small. The magnetizing current in the MFCS-II is higher than for a conventional Dual Active Bridge, and even for small voltages applied to the system, the current rises rather fast. These two small inductances therefore result in higher currents and thus higher losses in the dc-dc converter for the phase-shift modulation.

The modulation schemes have to fulfill several constraints, which are summarized in Table I. To avoid saturation of the transformer, it is necessary that the applied voltage has locally a zero-mean value. This restriction means for the fourth leg, which compensates the average value of the zero-sequence voltage, that the relative off time δ_{s4} of s_4 is determined by the zero-sequence voltage and thus the inverter's switching states. Using the definition of the zero-sequence voltage $v_z = \frac{V_{in}}{3}(\overline{s_1} + \overline{s_2} + \overline{s_3})$, it follows that $\delta_{s4} = \frac{1}{3}(\delta_{s1} + \delta_{s2} + \delta_{s3})$. Further, the voltage on the secondary side of the transformer has to have zero-mean. There might be several possibilities for the relative on times to guarantee this, but because they cause all the same losses, the relative off times δ_{st1} and δ_{st2} of s_{t1} and s_{t2} have been determined to be 50 percent in steady-state operation for simplicity.

In addition to these restrictions on the relative on time of the switches, it has to be assured that the desired output power is achieved. To do so, the steady-state currents, their rms values and the transferred steady-state power are calculated for each of the presented modulation schemes by forming Fourier series of the three voltages v_z, v_{s4} and v_t [1].

Keeping these constraints, there are several possible modulation schemes.

To analyze efficiency of the modulation schemes, the losses are split up in conduction and switching losses. The conduc-

tion losses P_c are proportional to the squared rms-value, i.e. $P_c = c_1 i_{rms}^2$, and the switching losses P_s are depending on the turn-on/off currents, i.e. $P_s = c_2 i_{turnoff}$, where a decreased current results in lower losses (as long as soft switching is guaranteed). Since the efficiency is not only depending on the total losses but also on the transferred power, it is useful to scale these losses by dividing them by the output power P_{out}. The advantage of this scaling becomes more clear if we rewrite the efficiency as

$$\eta = \frac{P_{out}}{P_{in}} = \frac{P_{out}}{P_{out}+P_c+P_s} = \frac{1}{1+\frac{P_c}{P_{out}}+\frac{P_s}{P_{out}}} = \frac{1}{1+c_1\frac{i_{rms}^2}{P_{out}}+c_2\frac{i_{turnoff}}{P_{out}}}.$$

Therefore, the scaled loss parameters give direct information of their influence on the efficiency.

It can be seen that the actual loss-parameters depend on the chosen system and the operating point. Nevertheless, the implemented algorithms optimize the total efficiency and are thus applicable for any operating point and system. For example, these algorithms can also be applied to the conventional Dual Active Bridge.

To illustrate the general statements, the working point with input voltage V_{in}=200 V, output voltage V_{out}=14 V, and rotational speed n=150 rpm is chosen for the MFCS-I. The zero-sequence current and the turn-off current of the switch s_4, which are essential for the prototypes efficiency, are shown here. Figure 3 depicts the scaled squared rms-value of the zero-sequence current and the scaled turn off current of switch s_4 against the output power for the phase-shift and an optimized modulation scheme, which are described amongst others in the following.

1) Phase-Shift Modulation: In phase-shift operation [14], the low voltage rectifier is controlled so that half the time switches s_{t1} and $\overline{s_{t2}}$ are closed and the other half switches $\overline{s_{t1}}$ and s_{t2}. Furthermore, the voltage across the lower switch s_4 of the fourth leg is controlled to be symmetrical with respect to $\omega_s t = \pi$ where ω_s is the angular switching frequency. There, the zero-sequence voltage v_z is used for the time and angle reference. The time/angle shift of the rectifier voltage $v_t = v_{t1} - v_{t2}$ relating to the reference is referred to as phase-shift φ. Figure 4(a) illustrates the converter waveforms for phase-shift operation.

It is obvious from Figure 3 that the relative losses increase excessively for power transfers considerably smaller than the maximum achievable output power P_{max}. On one hand, the ratio of reactive power to output power increases, thus increasing the conduction losses. On the other hand, this relative increase of the reactive power also increases the turn on/off currents, thus increasing also the switching losses.

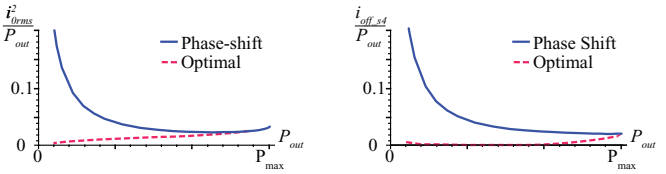

(a) Ratio of the squared rms current i_0 to the transferred power in dependence on P_{out}

(b) Ratio of the the turn-off current i_0 for s_4 to the transferred power in dependence on P_{out}

Figure 3: Loss parameters for the prototype system with input voltage V_{in}=200 V, output voltage V_{out}=14 V, rotational speed n=150 rpm.

2) Optimal Modulation: To improve the efficiency in the lower power regions, an improved modulation scheme has been developed. In phase-shift operation, the phase angle φ_{s4}, representing the relative phase-shifts between the zero-sequence voltage v_z and the fourth-leg voltage v_{s4}, is fixed to π. Furthermore, the relative phase-shift φ_{t2} between v_z and the voltage v_{t2} across s_{t2} is fixed to $\varphi_{t1}+\pi$. For the maximum power, there is no possibility to increase the total efficiency for a given system, as all the phase angles are determined. But for smaller powers, several phase angle combinations leading to the desired power can be found, thus offering the possibility to improve the efficiency. The optimal modulation takes advantage of this option. In the optimal modulation (see Figure 4(b)), φ_{s4} and φ_{t2} are optimized for minimal losses with the constraints for the modulation function as shown in Table I. In other words, for given input voltage, output voltage, and output power, the efficiency is optimized. Figure 3 illustrates the decrease of the rms-current and the turn off currents (dotted) compared to the phase-shift modulation (solid).

3) Multiple Switching: Another possibility to improve the efficiency is to switch the switches of the fourth leg and/or the secondary side legs more than once during a switching period of the inverter. Figure 4(c) shows the converter waveforms for a tripple-switching of s_4. Again, this switching scheme is only applicable for power transfers smaller than the maximum power. But for smaller powers, the total relative off time δ_{s4} of s_4 can be distributed to several off times, thus offering the possibility to improve the efficiency. In the multiple switching modulation with an x-times switching, the turn on and off times $b_1 ... b_{2x}$ are optimized for minimal losses with the constraints shown in Table I.

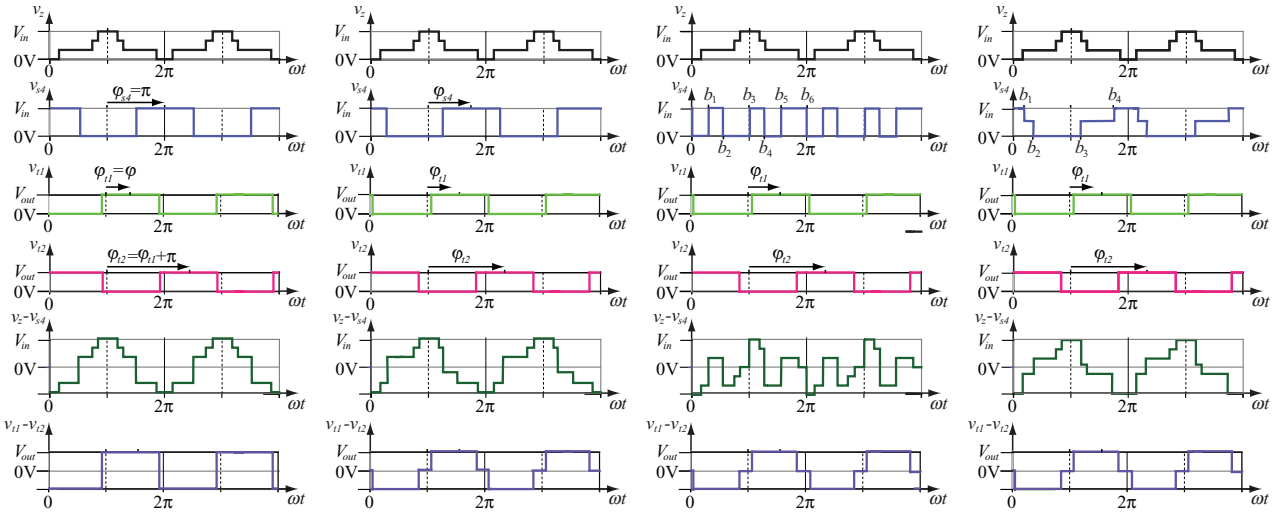

(a) Phase-Shift (b) Optimal (c) Multiple Switching of s_4 (d) Three-Level

Figure 4: Schematic converter waveforms: zero-sequence voltage v_z, voltage v_{s4} across s_4, voltage v_{t1} across s_{t1}, and voltage v_{t2} across s_{t2}.

As the turn-on/off currents are smaller for this modulation, the switching losses do not increase necessarily or might even decrease. The smaller rms-currents reduce the conduction losses, thus decreasing the total losses for certain operating points. Nevertheless, the application of this modulation scheme makes in general only sense if the conduction losses are significantly higher than the switching losses.

4) Three-Level Switch: To implement the fourth leg as a three-level switch is another possibility to improve the converter's efficiency. The three-level switch allows the voltage v_{s4} in Figure 1 to take values of not only 0 and the input voltage V_{in} (relating to the negative bus bar), but also half the input voltage, i.e. $V_{in}/2$. The time for which v_{s4} equals V_{in} during a switching period is denoted as $\delta_{Vin}T_s$ and the time for which v_{s4} equals $V_{in}/2$ is denoted as $\delta_{Vin/2}T_s$, where T_s is the inverter's switching period. As described in Table I, the fourth leg has to compensate the mean value of the zero-sequence voltage, i.e. $\frac{V_{in}}{3}(\delta_{s1}+\delta_{s2}+\delta_{s3}) = V_{in}\delta_{Vin} + \frac{V_{in}}{2}\delta_{Vin/2}$ or $\frac{1}{3}(\delta_{s1}+\delta_{s2}+\delta_{s3}) = \delta_{Vin}+\frac{1}{2}\delta_{Vin/2}$. For powers smaller than the maximum power, several combinations of δ_{Vin} and $\delta_{Vin/2}$ satisfying this sum and leading to the desired power can be found, thus offering the possibility to improve the efficiency. In the three-level switch modulation, the turn on and off times $b_1 ... b_4$ are optimized for minimal losses with the constraints for the modulation function as described in Table I. Figure 4(d) shows the converter waveform for this setup. It is also possible to combine the three-level switch with the multiple switching modulation, increasing the degree of freedom even more. Since this system would be even more complex and thus increasing the size of the look up table without increasing the efficiency considerably, this possibility is not discussed in this paper.

Table II: Comparison of the four modulation strategies.

Strategy	Hardware	Software
Phase-shift	No additional	No additional
Optimal	No additional	Look up table for 3 parameters
Multiple switching	No additional	Look up table for 1+2s parameters
Three-level switch	Three-level switch for the forth leg	Look up table for 5 parameters

5) Comparison of the four modulation strategies: In the following, the different switching strategies are compared regarding hardware and software complexity, efficiency and area of application. The phase-shift modulation is very easy to implement, but the system's efficiency decreases significantly for power transfers smaller than the maximum power. For the other modulations schemes, the switching instants are stored in a lookup table. The inverter's switching times are given. Since the total on/off times are also given, one switching instant for each leg can be calculated and has not to be stored. Additionally, the optimized times between two operating points are fairly linear, thus allowing to limit the number of entries. If a feed forward control is used, 3 parameters have to be stored for the optimal modulation. If one leg is switched x times for

Table III: Parameters of the prototype.

Parameter	Value
# poles	8
nominal speed	1500 rpm
input voltage V_{in}	200 V...400 V
motor power	9.4 kW
back EMFs e_R, e_S and e_T	67.8 Vrms at 1000 rpm

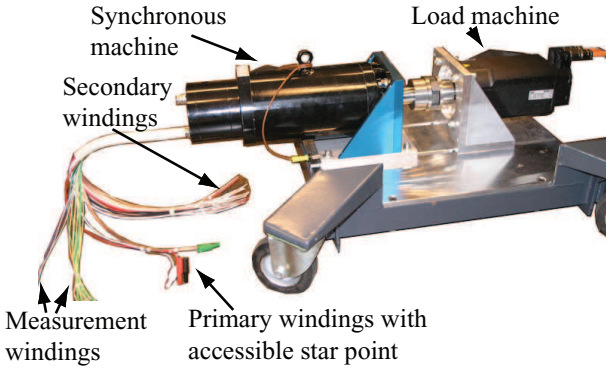

Figure 5: Prototype motor with accessible star point (and secondary windings for MFCS-II).

Figure 6: Converter System.

the multiple switching modulation, $2x$-1 parameters have to be stored for this leg plus 2 parameters for the other two legs of the dc-dc converter. For the three-level system, 5 parameters have to be stored. As opposed to the other modulations, where the hardware is not affected, one leg has to be modified to a three level switch for the last modulation. As long as the efficiency is tolerable high, the first two strategies are thus superior to the others since they do not need any additional hardware and since they have the smallest software effort. Table II summarizes the comparison.

B. Design and Experimental Results of MFCS-I

A synchronous motor with accessible star point with the parameters given in Table III has been designed to validate the proposed MFCS-I. The prototype shown in Figure 5 has also

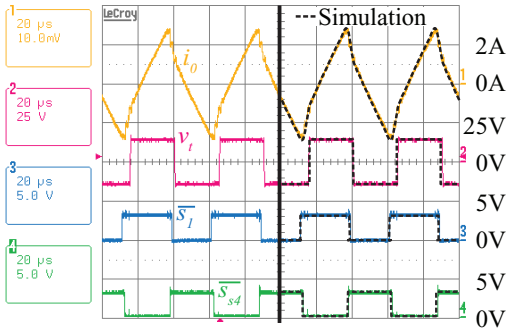

(a) Phase-Shift

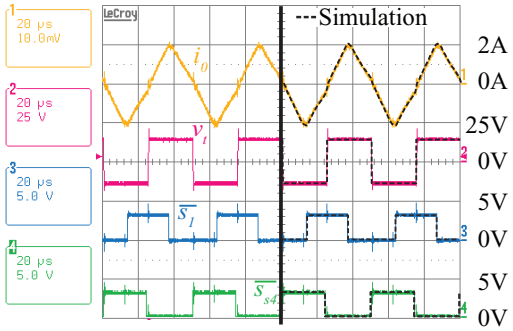

(b) Optimal

Figure 7: Measurement and simulation results obtained with the test system. There, the input voltage V_{in}=200 V, output voltage V_{out}=14 V, transferred power $p_{dc-dc} = 0.6P_{max}$, rotational speed n=150 rpm.

Figure 8: Efficiencies.

Phase-Shift	56
Optimal	67
Multi	69
Three-Level	72

integrated secondary windings in order to allow the evaluation of MFCS-II.

The converter system presented in Figure 6 includes not only an inverter to drive the motor, but also a dc-dc converter as shown in Figure 1(b) and (c) with the legs leg$_4$, leg$_{t1}$, and leg$_{t2}$. To validate the three-level modulation, the fourth leg is also implemented as a three-level switch.

The target system is based on a 50 kW machine, the dc-dc converter having a nominal power of 1 kW. Scaling the system down to the 9.4 kW prototype machine results in a dc-dc converter with a nominal power of 188 W.

Both the MFCS-I and MFCS-II have been taken into operation and they function properly with phase-shift modulation as shown in [1] and [11] respectively. For this paper, the new modulation schemes have been implemented and tested. Figure 7 show the measurements for the operation of the MFCS-I for phase-shift (a) and optimal modulation (b). The machine rotates at 150 rpm with an input voltage of 200 V

and an output voltage of 14 V. The dc-dc converter transfers 60% of the maximum output power. It is obvious that the primary side rms current is smaller for the optimal modulation and thus, in consequence of the relatively high zero-sequence impedance, the efficiency is improved to 67% with the optimal switching scheme, compared to 56% for the phase-shift scheme. Furthermore, the measurements agree very well with the simulations (dotted lines), which where performed with the model presented in Subsection II-A. Since the zero-sequence resistance of the prototype is rather large, the efficiencies are smaller than for normal dc-dc converters. Electrical machines used in hybrid cars usually have higher power ratings than the prototype machine. The relative resistance (i.e. the per-unit resistance) decreases with machine size, and so do the relative resistive losses as well as the relative iron losses. Therefore, the zero-sequence resistance for machines intended for hybrid vehicles is smaller than that of the prototype machine even for high frequencies, which means that the losses decrease and the efficiency increases significantly for the real application [1]. To have an estimate of the efficiency of the target system, the zero-sequence impedance of a 50 kW motor used in a hybrid car has been measured. Appropriate switches have been chosen. The calculations showed that an efficiency of 87% and more can be reached for an output power larger than $0.6P_{max}$.

Table 8 summarizes the efficiencies of the dc-dc converter of the prototype for all modulation schemes for 60% of the maximum output power.

III. Conclusion

The total system costs and weight can be reduced by integrating the dc-dc converter, which connects the low and high-voltage buses of a hybrid vehicle, into the traction inverter and the electrical machine. With the integration concept MFCS-I, the inverter and the machine are used to implement a primary bridge leg of an isolated full bridge dc-dc converter. The MFCS-II offers an even higher degree of integration, since it allows not only to replace one leg of the dc-dc converter by the inverter stage, but also to fully integrate the transformer in the machine. In this paper, new switching strategies to improve the efficiency of these two converter systems are presented and verified by simulations and measurements.

In order to validate the switching strategies a scaled prototype with a 9.4 kW machine and a dc-dc converter has been constructed. The resulting measurements agree very well with the simulations and the analytical models. Efficiencies of about 56 percent were measured for phase-shift operation and 67 percent for the optimal modulation. The efficiency can be increased with the multiple switching or the three-level scheme. For the target system, efficiencies of 87 percent and more can be achieved through these modulations.

References

[1] H. Plesko, J. Biela, J. Luomi, and J. W. Kolar, "Novel concepts for integrating the electric drive and auxiliary dc-dc converter for hybrid vehicles," in *Proc. APEC 2007 - Twenty Second Annual IEEE Applied Power Electronics Conference*, Feb. 25 2007–March 1 2007, pp. 1025–1031.

[2] A. Emadi, M. Ehsani, and J. Miller, "Advanced silicon rich automotive electrical power systems," in *Proc. 18th Digital Avionics Systems Conference*, vol. 2, 24-29 Oct. 1999, pp. 8.B.1–1–8.B.1–8.

[3] J. Wang, F. Peng, J. Anderson, A. Joseph, and R. Buffenbarger, "Low cost fuel cell converter system for residential power generation," *IEEE Transactions on Power Electronics*, vol. 19, no. 5, pp. 1315–1322, 2004.

[4] K. Moriya, H. Nakai, Y. Inaguma, H. Ohtani, and S. Sasaki, "A novel multi-functional converter system equipped with input voltage regulation and current ripple suppression," in *Conference Record of the 2005 Industry Applications Conference Fourtieth IAS Annual Meeting*, vol. 3, 2-6 Oct. 2005, pp. 1636–1642.

[5] S. J. Lee and S. K. Sul, "An integral battery charger for 4 wheel drive electric vehicle," in *Conference Record of the 1994 IEEE Industry Applications Society Annual Meeting*, vol. 1, 2-6 Oct. 1994, pp. 448–452.

[6] T. Franke, "Switching device for linking various electrical voltage levels in a motor vehicle," Patent WO/2006/105 840, October, 2006.

[7] S. Kinoshita, K. Fujita, and J. Ito, "Electric system for electric vehicle," Patent 6 066 928, May, 2000. [Online]. Available: http://www.freepatentsonline.com/6066928.html

[8] S. Sasaki, "Multiple power source system and apparatus, motor driving apparatus, and hybrid vehicle with multiple power source system mounted thereon," Patent 6 476 571, November, 2002. [Online]. Available: http://www.freepatentsonline.com/6476571.html

[9] J. M. Nagashima, D. S. Carlson, C. C. Stancu, S. Hit, and K. M. Rahman, "Auxiliary power conversion by phase-controlled rectification," Patent 6 617 820, September, 2003. [Online]. Available: http://www.freepatentsonline.com/6617820.html

[10] C. C. Stancu, S. Hiti, and J. Nagashima, "Auxiliary power conversion for an electric vehicle using high frequency injection into a pwm inverter," Patent 6 262 896, July, 2001. [Online]. Available: http://www.freepatentsonline.com/6262896.html

[11] H. Plesko, J. Biela, and J. W. Kolar, "Design and analysis of a new drive-integrated auxiliary dc-dc converter for hybrid vehicles," in *Conference Record of the 2008 IEEE Industry Applications Society Annual Meeting*, to be published in 2008.

[12] ——, "Drehstromantriebssystem mit hochfrequent potentialgetrennter bidirektionalen Kopplung der Versorgungsspannungen," Patent 01 220/06, 2006.

[13] J. Biela, H. Plesko, and J. W. Kolar, "Drehstromantriebssystem mit motorintegriertem Hochfrequenztrafo zur bidirektionalen Kopplung der Versorgungsspannungen," Patent 01 219/06, 2006.

[14] M. Kheraluwala, R. Gasgoigne, D. Divan, and E. Bauman, "Performance characterization of a high power dual active bridge dc/dc converter," in *Conference Record of the 1990 IEEE Industry Applications Society Annual Meeting*, vol. 2, 7-12 Oct. 1990, pp. 1267–1273.